Revista Minelor – Mining Revue
ISSN-L 1220-2053 / ISSN 2247-8590
vol. 30, issue 3 / 2024, pp. 1-21

THE SHELTERING EFFECT OF A CUDDY DURING A FIRE IN AN UNDERGROUND MINE

Rickard HANSEN[1*]

[1]Sweco AB, Stockholm, Sweden, rickard.hansen2@sweco.se

DOI: 10.2478/minrv-2024-0022

Abstract: *The most severe risk during a fire in an underground mine is the smoke spread, forcing the personnel to evacuate and take shelter. This study investigates the sheltering effect of a cuddy during a fire in an adjacent mine drift or a decline. The aim of the paper is to perform a parametric study on the sheltering effect, accounting for parameters such as the length of cuddy and ventilation velocity. Data from fire experiments in a model-scale mine drift and results from CFD simulations were used during the study. It was found that for a fire in an adjacent mine drift, extending the cuddy length resulted in the best conditions and increasing the heat release rate resulted in the worst conditions. An extended cuddy length will result in increased heat losses of the smoke layer. For a fire in an adjacent downslope decline, extending the cuddy length or increasing the ventilation velocity resulted in the best conditions. The increased ventilation velocity will cause an increased cooling of the smoke volumes entering the cuddy. An increased heat release rate resulted in the worst conditions. For the upslope decline case, extending the cuddy length resulted in the best conditions and increasing the heat release rate or increasing the ventilation velocity resulted in the worst conditions. An increased ventilation velocity in an upslope decline case will lead to larger portions of hot gases entering the cuddy.*
Keywords: *Smoke spread, mine drift, decline, stratification, CFD, mine fire, underground mine*

1. Introduction

A fire in an underground mine will present several risks and hazards to the mining personnel, and where the smoke spread – affecting the visibility and leading to intoxication - will constitute the major risk. During a fire underground, evacuation may take place depending on the severity of the fire, sensitive areas nearby, etc. Personnel underground may either evacuate to a position above ground or take shelter at a safe position underground, for example a refuge chamber. A fire underground will affect positions in a mine section differently, depending on parameters such as distance to the fire, the mass flow at the position, etc. A cuddy – defined in this study as a smaller drive off the side of the underground mine workings, where for example equipment or material can be stored or positioned and where no ventilation flow is forced into the drive – may provide extra protection for the evacuating mining personnel and refuge chambers, as the resulting mass flow situation and temperature distribution in the cuddy will be more favorable than in an adjacent mine drift or decline.

This paper investigates the mitigating effects of a cuddy during a fire in an underground mine and the parameters affecting the effectiveness of the cuddy as a shelter. How will the distance between the fire and the cuddy, the inclination and direction of the adjacent mine drift or decline, the longitudinal ventilation flow velocity, and the heat release rate of the fire affect the temperature distribution and smoke spread in the cuddy?

Understanding and knowing the impact of various influencing parameters on the sheltering effect of a cuddy will improve the safety of the underground personnel during the evacuation phase of an occurring fire underground.

The sheltering effect of a cuddy underground was investigated through a parametric study – focusing on the influence of various parameters - where a CFD (Computational Fluid Dynamics) tool was used to obtain data for the investigation. The input data for the CFD simulations were obtained from earlier model-scale fire experiments in a model scale mine drift where the heat release rate and the longitudinal flow velocity were varied in the experiments [1].

[*] Corresponding author: Rickard Hansen, Ph.D MSc Eng., Sweco AB, Stockholm, Sweden, rickard.hansen2@sweco.se

 vol. 30, issue 3 / 2024
pp. 1-21

The purpose of this paper is to investigate the conditions in a cuddy during a fire when varying several different influencing parameters.

Very few works have been conducted on the fire impact in dead-end areas off the side of the mine workings, and with a longitudinal ventilation flowing past the area or the drive. Edwards and Hwang [2] conducted a fire modelling study on the smoke spread from fires in a mine entry under zero airflow conditions. Thus, the study did not include the longitudinal ventilation flow in an adjacent mine drift or decline, and the fire was positioned in the mine entry where no ventilation flow existed. Friel et al. [3] conducted fire experiments and fire modelling (CFD tool) on smoke rollback through crosscut from return to an intake, where smoke-obscuration meters and thermocouples were positioned in crosscuts both upstream and downstream of the fire. The smoke-obscuration meters and thermocouples were positioned approximately 5 m into each crosscut. The heat release rates of the fire experiments were small for full-scale fire experiments – i.e., 500 and 660 kW – and any extensive conclusions are difficult to draw. Jaszczur et al. [4] studied air flow phenomena in a model-scale blind drift, where a ventilation flow into the blind drift was provided. No fire was added in the experiments. Chen et al. [5] conducted fire experiments in a model-scale bifurcated tunnel, where the position of the fire vis-à-vis the bifurcated point and the ventilation flow velocity was varied. At low flow velocities in the branch (approximately 0.6 m/s) and when the fire was positioned at the bifurcated point and thus adjacent to the branch, the temperature at the ceiling level and at the bifurcated point was measured at approximately 750°C, in the branch and 10 m from the bifurcated point at approximately 200°C and 20 m from the bifurcated point at approximately 150°C. At longer distances, the temperature started to level off more and more. When the fire was positioned 30 m upstream of the bifurcated point and the flow velocity in the main tunnel was 3.2 m/s, a temperature decrease from approximately 140°C at the bifurcated point to approximately 50°C 10 m into the branch resulted. The temperature decrease was significant – more than halved – if comparing the temperature in the main tunnel downstream of the fire and the temperature 10 m into the branch. As opposed to a cuddy, a longitudinal ventilation flow was provided in the branch.

No earlier in-depth study has dealt with the sheltering effect of a cuddy during a fire in an underground mine.

In the ensuing chapters, the smoke spread and temperature distribution in a mine drift or a decline with a burning object and longitudinal ventilation flow are described. Earlier performed model-scale fire experiment and the set-up of the CFD simulations – with included input data - are described. The resulting simulation results are analysed and discussed, foremost focusing on the environment in a cuddy and the influence of various parameters.

2. Temperature distribution and smoke spread in a mine drift or a decline during a fire

The temperature distribution and smoke stratification in the adjacent mine drift or decline to the cuddy will have a large impact on the environment in the cuddy, as the mine drift and decline conditions will be the source for the temperature and smoke spread conditions in the cuddy. Thus, any changes occurring in the mine drift or decline will greatly affect the ensuing conditions and environment in the cuddy.

The temperature distribution in a mine drift during a fire will visibly be closely connected to the occurring smoke stratification. In the near vicinity and downstream of the fire, the smoke stratification will be significant and the vertical temperature gradient high (with very high temperatures in the upper region of the mine drift and much lower temperatures at the lower region). With increasing heat release rate, the smoke stratification and the temperature gradient will be high at an increasing distance from the fire. With increasing ventilation flow velocity, the temperature gradient downstream will be low at a decreasing distance from the fire. At sufficiently long distance from the fire, the smoke stratification will be negligible and the temperature more or less uniform across the mine drift. See Fig. 1 for the varying smoke stratification and temperature gradient along a mine drift.

The smoke spread in a mine drift will be highly transient, both in time and spatially. The spatial variations can be seen both with increasing distance from the fire as well as upstream versus downstream of the fire. Initially, the smoke will rise and spread in the direction of the ventilation flow, but as the heat release rate increases an inflow of air towards the base of the fire and a counter-current flow of smoke at the upper region and downstream of the fire will occur. The counter-current flow of hotter smoke will start to cool off as it mixes with the cooler ventilation air flowing in the opposite direction and start to descend towards the floor and subsequently veer back towards the fire region. Further downstream of the fire, the multi-directional flow will become a uni-directional flow. With increasing heat release rate, the downstream distance to uni-directional flow will increase. With increasing ventilation flow velocity, the distance to uni-directional flow will decrease. Fig. 1 displays the schematic mass flows in a mine drift with longitudinal ventilation flow.

vol. 30, issue 3 / 2024
pp. 1-21

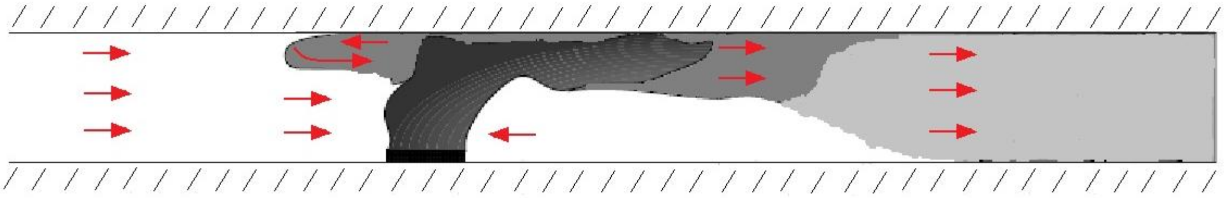

Fig.1. Schematic temperature distributions and mass flows (mass flow directions marked by red arrows) in a mine drift with longitudinal ventilation flow [6]

In a decline, the temperature distribution and smoke spread will depend on – other than the heat release rate and ventilation flow velocity – the degree of inclination and the direction of the decline versus the direction of the ventilation flow.

With a downslope fire scenario – i.e., longitudinal ventilation flowing downwards along the decline and with a fire occurring at the upper part – a greater degree of turbulence, mixing and a lower degree of smoke stratification can be expected compared with no inclination. The scenario will be distinguished by a longitudinal ventilation flow in one direction and a buoyant flow from the fire in the opposite direction. The counter-current flow of hotter smoke at the upper region will be higher compared with the horizontal, mine drift case. An increased turbulence and mixing will result in a shorter stratification region downslope of the fire and shorter distance to uniform gas temperatures and uni-directional flow in the vertical direction. Wu et al. [7] conducted fire experiments in a sloped model-scale tunnel and found that the fire gases cooled rapidly and an increasingly uniform cross-sectional gas temperature with increasing inclination. With an increased inclination, the turbulence will increase, and the length of the stratification region decrease even further. Furthermore, with a downslope fire scenario a thicker smoke layer can be expected.

With an upslope fire scenario – i.e., longitudinal ventilation flowing upwards along the decline and with a fire occurring at the lower part - less turbulence can be expected compared with the downslope scenario as the longitudinal ventilation and the buoyant smoke would flow in the same direction. If comparing with the downslope scenario, an upslope scenario would result in less mixing, a slower temperature decay of the smoke and a longer stratification region downstream of the fire. If comparing with a mine drift with no inclination, an increasing inclination in an upslope fire scenario would lead to an increased velocity of the flowing smoke and an increased turbulence. With an increasing turbulence, the length of the stratification would decrease. The counter-current flow of hotter smoke at the upper region will be less significant – if occurring at all - compared with the horizontal, mine drift case.

Fig. 2 displays the smoke stratification and temperature distribution for the downslope scenario and upslope scenario.

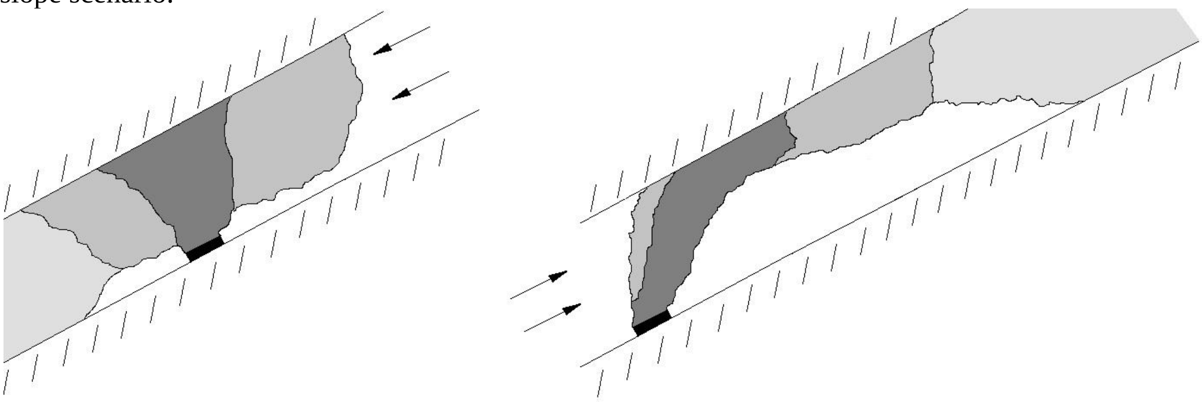

Fig.2. The smoke stratification and temperature distribution for the downslope scenario (left) and upslope scenario (right) in a decline

3. Methodology

Initially, data from an earlier model-scale fire experiment in a model mine drift was obtained and from which a number of base cases were derived from. In the base cases a cuddy was added in all cases and a decline with varying direction was applied in two of the base cases. The CFD tool had earlier been validated against this specific model-scale experimental results [8]. During the ensuing investigative CFD simulations, the base cases were applied and where the heat release rate, the distance between the fire and the cuddy, the longitudinal flow velocity, the degree of inclination, and the length of cuddy were varied.

 vol. 30, issue 3 / 2024
pp. 1-21

3.1 Fire experiment in a model-scale mine drift

The cost and resource intensive nature of full-scale fire experiment is often observed, whereas model-scale fire experiments offer advantages in terms of being more cost effective as well as providing resources efficiently. In order to investigate the fire spread and fire behavior of a single and multiple fuel items along a mine drift, a model-scale mine drift was used for twelve fire experiments. The model-scale mine drift was horizontal with no inclination. The fuel items in the experiments were made up of either a single pile of scaled wooden pallets or several piles placed at pre-determined positions. Fig. 3 displays a scaled-down wooden pallet applied in the experiments. In all experiments - where the flow velocity was set to 0.3, 0.6 or 0.9 m/s - a longitudinal ventilation flow was established during each experiment. Three experiments were conducted with a single pile of wooden pallets. The difference between the three experiments was found in the ventilation flow velocity, i.e., 0.3 m/s, 0.6 m/s or 0.9 m/s. The mine drift was measured at scale 1:15, 10 m in length, 0.6 m in width and 0.4 m in height. Fig. 4 shows a long-section layout of the model scale mine drift, consisting of two piles of wooden pallets with attached thermocouples, probes and other measuring devices. The measuring devices of interest in this specific study would be the thermocouple pile named “pile B” (where the vertical temperature downstream of the fire would be measured) and the upstream and downstream bi-directional probes which provided the average ventilation velocities upstream and downstream of the fire (it was later found that the upstream bi-directional probe registered erratic values due to increased eddy formations during fires and therefore the measured average ventilation velocity prior to the fire was used as the input ventilation velocity in the simulations).

Fig.3. A scaled-down wooden pallet used as fuel item in the fire experiments

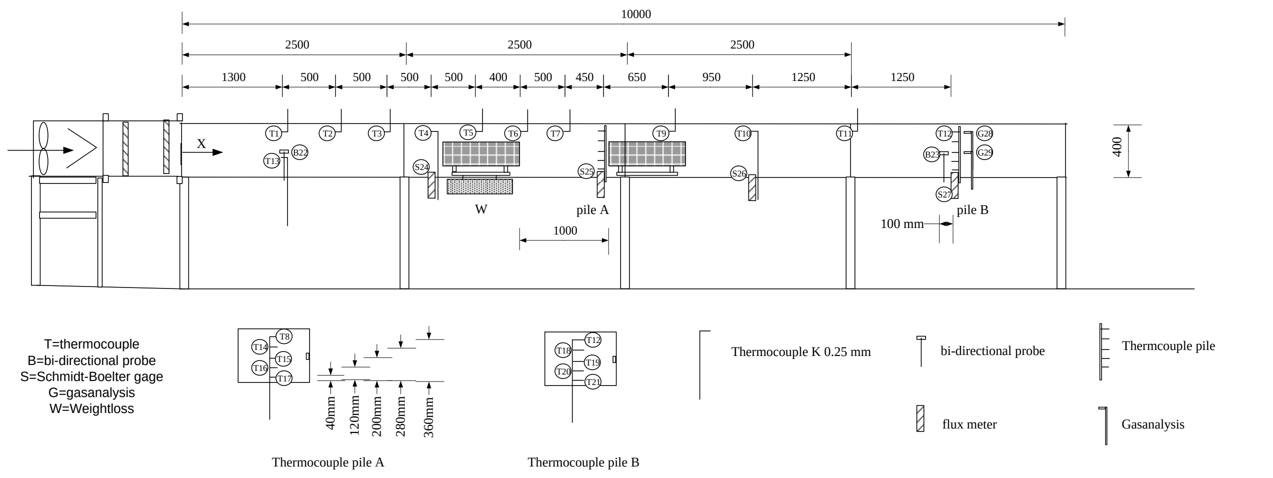

Fig.4. The long-section layout of the model-scale mine drift with the positions of various measuring devices [9]

Fig. 5 displays the resulting heat release rate curve of the experiment involving a single pile of pallets and a ventilation flow velocity of 0.3 m/s.

For more in-depth descriptions of the experiments and the measurements recorded, see report by Hansen and Ingason [9].

vol. 30, issue 3 / 2024
pp. 1-21

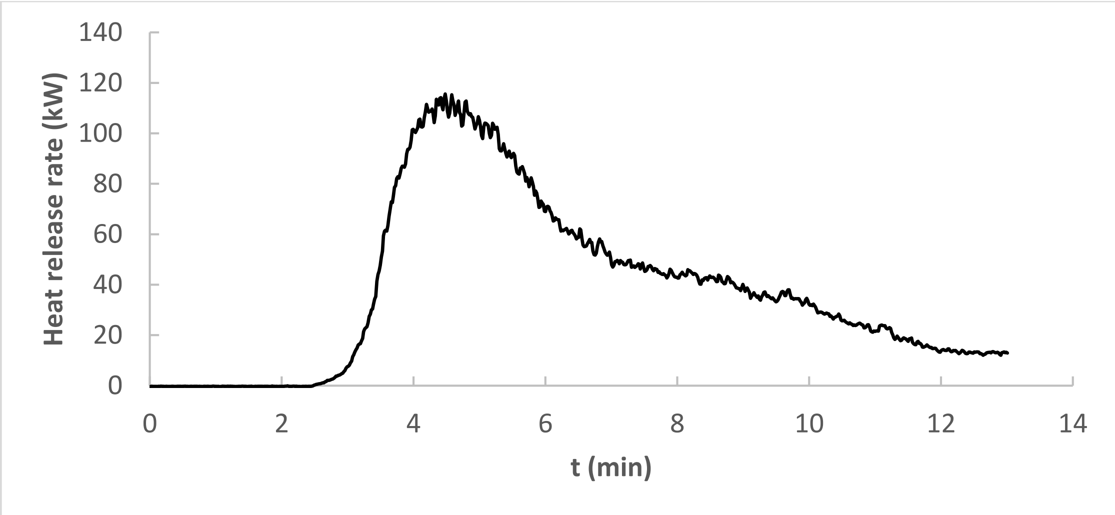

Fig.5. The heat release rate of the experiment with a single pile of wooden pallets and a longitudinal ventilation flow velocity of 0.3 m/s

3.2. CFD simulations

Due to its ability to model complex geometries and fire characteristics, CFD models are commonly used for modelling and predicting parameters such as ventilation flow and heat transfer during fires.

In view of the time consuming and demanding nature of CFD modelling in computational resources with an increasing size of a modelled domain, any simulation will be carried out on a limited part of the mine. The computational domain is divided into a 3D mesh of multiple cells by a CFD model. Fundamental laws of fluid mechanics and heat transfer, as defined by the laws of conservation mass, momentum and energy, are applied to each cell. For further background on CFD modelling of fires, see publication by Yeoh and Yuen [10].

A CFD model was applied in an earlier study where the throttle effect in an underground mine was investigated. During the study the simulation results were analysed and validated against the experimental data from the model-scale fire experiments [8]. The CFD model in question was version 6.7.5 of the Fire Dynamics Simulator (FDS). During the study it was found that a single measuring point to model the downstream flow velocity - i.e., the bi-directional probe at thermocouple pile B (see Fig. 4) – led to uncertainties and large differences in the simulation results compared with the experimental results as the variations along the cross-section would not be accounted for. If instead applying multiple measuring points downstream in the model and calculating an average flow velocity, the uncertainties and differences were reduced significantly. For further reading on the assumptions made, parameters applied, findings and results when applying a CFD model in a mine section, see paper by Hansen [8].

The specific parameter and model-scale experiment selected for validation was the mass flow rate for the experiment involving a single pile of wooden pallets and a longitudinal ventilation velocity of 0.3 m/s. The measured and the modelled mass flow rate downstream of the fire at thermocouple pile B can be seen in Fig. 6. The mass flow rate contains the temperature as well as the flow velocity and will therefore be of high interest when validating the temperature distribution and the smoke spread. The specific experiment was selected as thermocouple pile B and the downstream bi-directional probe were found to be downstream of the hydrodynamically fully developed region in this experiment and a single pile of wooden pallets would allow for an accurate determination of the heat release rate of the pile. The modelled mass flow rate in Fig. 6 can be seen to match the experimental and measured mass flow rate very well except for the latter part of the simulation. In the analysis it was found that the mass flow rate in the experiment most likely matched the modelled mass flow rate during the latter part well but that the single bi-directional probe resulted in too high mass flow rates [8]. The confidence in the modelling results thus increased. Even though the modelled results matched the experimental results very well, deviations remain and in the following analysis the results from the CFD model will be studied taking a qualitative approach.

Based on the findings in the fire modelling paper by Hansen [8], the simulations in this study are largely based on identical input data as in the modelling study. The only differences can be found in the use of the HVAC (Heating, Ventilation and Air Conditioning) feature, the applied CFD model version (version 6.9.1 of FDS was applied in the current study), and the inclusion of a cuddy and declines in some cases. The HVAC feature will simplify the simulations and decrease the run time as well. For further details on the HVAC feature in the fire modelling of the model-scale mine drift, see paper by Hansen [6].

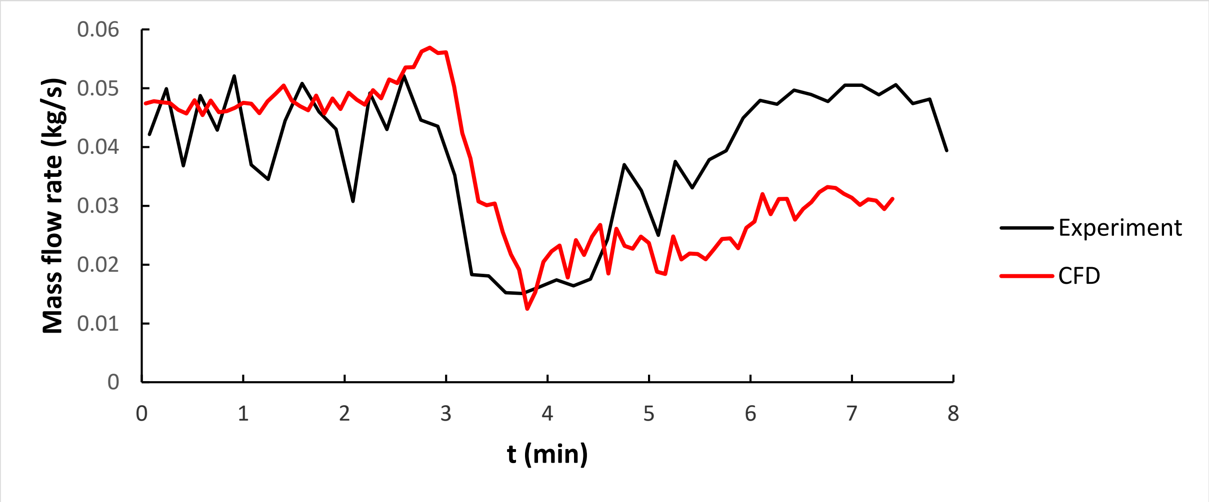

Fig.6. The experimental measured and the modelled mass flow rate downstream of the fire for the model-scale experiment involving a single pile of wooden pallets and a longitudinal ventilation velocity of 0.3 m/s [6]

A cuddy was positioned two meters downstream of the burning pile of wooden pallets in the base cases. The cross-sectional dimensions of the cuddy were 0.3 m in height and 0.3 m in width. The length of the cuddy was 3 m in the base cases. In some ensuing simulations the position of the cuddy versus the fire and the length of the cuddy were varied.

In the base cases where a decline was investigated, the inclination was 5% for the upslope case as well as the downslope case. In some ensuing simulations the inclination of the decline was varied.

The mesh grid size in the study by Hansen [8] was 0.02 m, which was also applied in this study.

The investigated and varied influencing parameters were the heat release rate, the distance between the fire and the cuddy, the longitudinal flow velocity, the degree of inclination, and the length of cuddy.

The temperature, visibility, and mass fraction of carbon monoxide and carbon dioxide were measured in the cuddy applying slice files or point measurements to obtain the variations along the cuddy. The four parameters were selected as they are commonly used as tenability criteria when evaluating the safety for the personnel [11].

4. Results and discussion

In the ensuing chapters the results and analysis on the base cases (involving a mine drift, a downslope decline case, and an upslope decline case), the impact of the distance between the fire and the cuddy, the heat release rate, the longitudinal flow velocity, the degree of inclination, and the length of cuddy on the visibility, temperature, and mass fractions of gases in the cuddy can be found.

The results of the CFD simulations are presented as point measurements or slice files displaying the variations along the length of the cuddy and the cross-section of the mine drift or decline in level with the cuddy. The following points in time were selected for the analysis of the slice files: 280 s into the simulation which would capture the effects of the maximum heat release rate (see Fig. 5); 380 s into the simulation which would constitute an intermediate time point; 480 s into the simulation which constitutes the end of the simulation.

In the ensuing chapters comparison and discussion on equivalent full-scale parameters can be found, applying the following equations when calculating the corresponding full-scale value [12-13]:

Heat release rate: $$\dot{Q}_F = \dot{Q}_M \cdot \left(\frac{L_F}{L_M}\right)^{5/2} \quad (1)$$

Flow velocity: $$u_F = u_M \cdot \left(\frac{L_F}{L_M}\right)^{1/2} \quad (2)$$

Time: $$t_F = t_M \cdot \left(\frac{L_F}{L_M}\right)^{1/2} \quad (3)$$

Temperature: $$T_F = T_M \quad (4)$$

where $\dot{Q}$ is the heat release rate [kW], u is the flow velocity [m/s], L is the length [m], t is the time [s], and T is the temperature [K].

The index F relates to the full-scale (i.e., 15 in this case) and the index M relates to the model-scale (i.e., 1 in this case). A model-scale length of 1 m in the model-scale experiments would therefore be equivalent to 15 m in full-scale.

As can be seen in equation (4), the model-scale temperature is directly equivalent to the full-scale temperature. The corresponding full-scale heat release rate of the base cases would be approximately 25 MW, which corresponds to a fully developed fire in a larger mining vehicle. The full-scale distance between the fire and the entrance to the cuddy would be 30 m, the full-scale length of the cuddy would be 45 m, and the full-scale ventilation velocity would be approximately 1.2 m/s.

4.1 Base cases

Mine drift

Fig. 7 displays the temperature variations at the entrance, half-way and at the end of the cuddy (the initial two minutes are not shown as the fire was initiated after two minutes). As noted, the temperature differences between the floor and the ceiling will be highest at the entrance and with very little temperature differences at the end of the cuddy. This difference in temperature stratification can also be seen in the slice file in Fig. 8. The highest temperatures at the time of the peak heat release rate can be seen at the ceiling level at the entrance and half-way into the cuddy - i.e. in the 50-60°C range – the lowest temperatures can be found at the floor level at the entrance and half-way into the cuddy – i.e., approximately 25°C. The temperatures at the remaining positions are found in the interval 30-40°C. At the end of the simulation the average temperature at the ceiling level at the entrance and half-way into the cuddy is approximately 40°C, the average temperature at the remaining positions – except at the floor level at the entrance and half-way into the cuddy – is approximately 30°C.

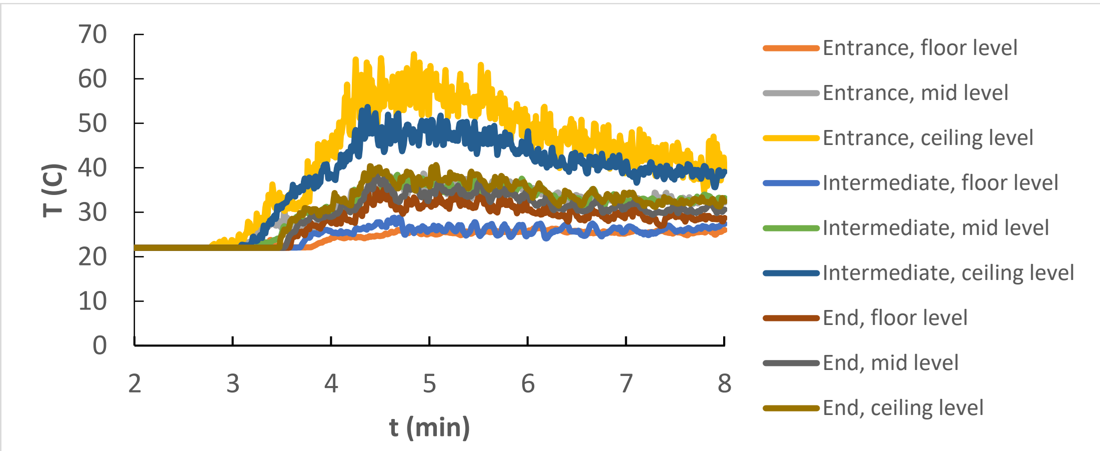

Fig.7. The temperature variations at the entrance, intermediate and end of cuddy at three different heights

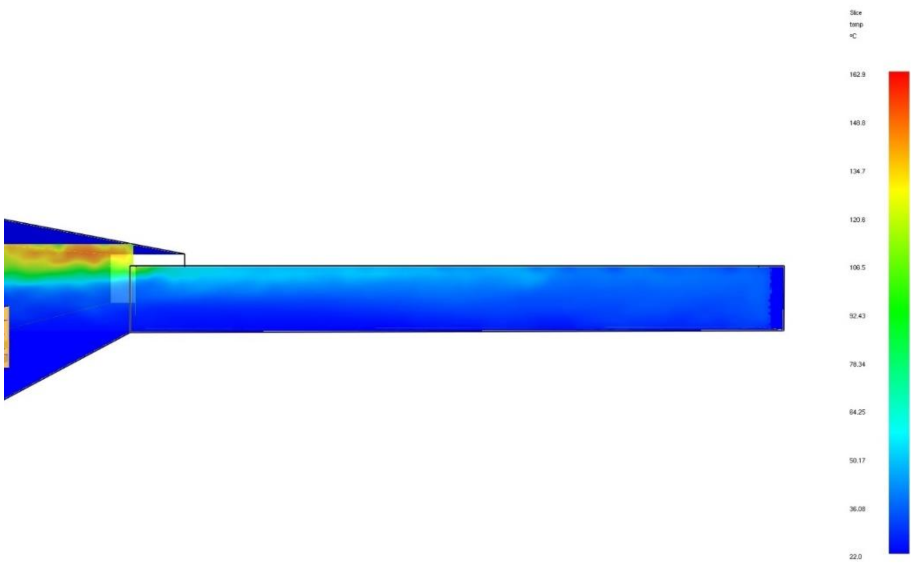

Fig.8. Slice file displaying the temperature variations along the cuddy and in the mine drift at t=280 s; the mine drift can be seen to the left and the full length of the cuddy perpendicular and originating from the mine drift

 vol. 30, issue 3 / 2024
pp. 1-21

Fig. 9 displays the variations in visibility along the cuddy. As seen, except for the floor level at the entrance (due to a higher degree of stratification), the visibility quickly drops to 10 meters or below approximately three minutes after the start of the fire (which corresponds to approximately 12 minutes for a full-scale scenario). The minimum visibility was approximately 8 m. For comparison, a visibility of at least 10 meters is a frequently applied criterion when evacuating buildings or tunnels [14-15]. The poor visibility conditions remain at most positions throughout the entire simulation. Except for the ceiling level at the cuddy entrance, the smoke will thus still linger. The end of simulation (t=480 s) corresponds to approximately 31 minutes for a full-scale scenario.

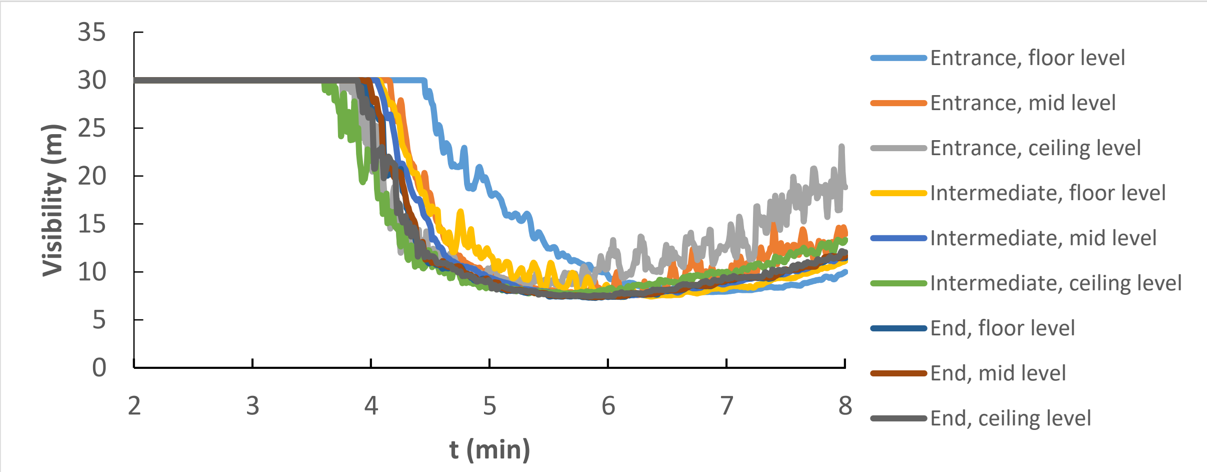

Fig.9. The variations in visibility at the entrance, intermediate and end of cuddy at three different heights

Fig. 10 displays the variations in CO mass fractions along the cuddy. As the mass fraction is a dimensionless parameter, the full-scale results will be identical with the modelled model-scale results. The variations in the CO mass fractions will correlate with the visibility found in Fig. 9. The variations of the CO_2 mass fraction are identical with the CO mass fraction but with a different magnitude. The peak CO mass fraction at approximately $2.0 \cdot 10^{-5}$ corresponds to 20 ppm, whereas the peak value was approximately 0.01 for the CO_2 mass fraction which corresponds to 10 000 ppm. As opposed to the visibility, the CO mass fraction will clearly decrease at the end of the simulation with values below $1.5 \cdot 10^{-5}$ for most positions.

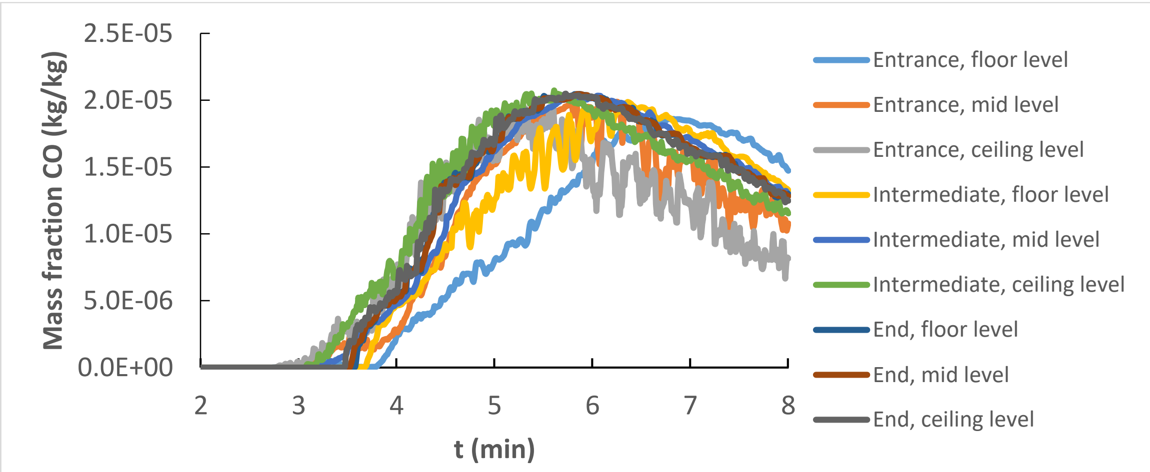

Fig.10. The variations in CO mass fraction at the entrance, intermediate and end of cuddy at three different heights

Downslope decline

The modelled temperatures for the downslope decline scenario can be found in Fig. 11. The temperature distribution is similar to the temperature distributions for the horizontal mine drift scenario (see Fig. 7). The difference can be found in the magnitude of the temperatures, where the temperatures in the cuddy for the downslope decline case is higher than for the mine drift case.

The highest temperatures at the time of the peak heat release rate can be seen at the ceiling level at the entrance – approximately 100°C - and half-way into the cuddy – approximately 80°C – the lowest temperatures can be found at the floor level at the entrance and half-way into the cuddy – approximately 40°C. The temperatures at the remaining positions are found in the interval 45-60°C. The slice file in Fig. 12 displays the

vol. 30, issue 3 / 2024
pp. 1-21

generally higher temperatures in the cuddy but also the hotter gas temperatures in the decline at lower levels (caused by the increased turbulence and lower degree of stratification), which will lead to hotter gas volumes entering the cuddy. At the end of the simulation the average temperature at the ceiling level at the entrance and half-way into the cuddy is approximately 60°C, the average temperature at the floor level at the entrance and half-way into the cuddy is approximately 35°C, and the temperature at the remaining positions is approximately 45°C.

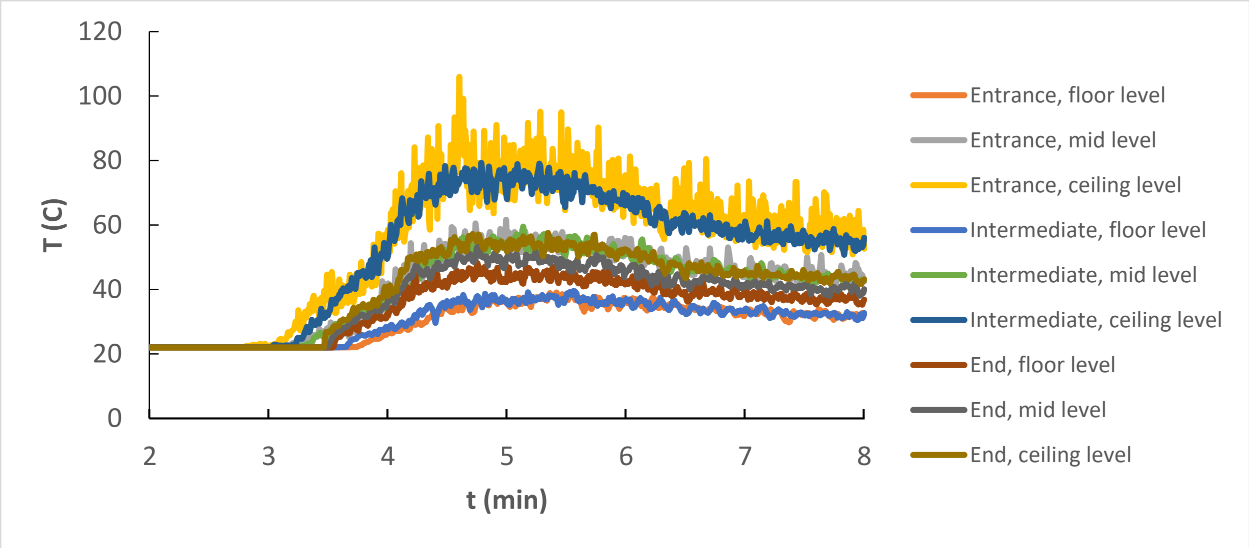

Fig.11. The temperature variations at the entrance, intermediate and end of cuddy at three different heights – downslope decline case

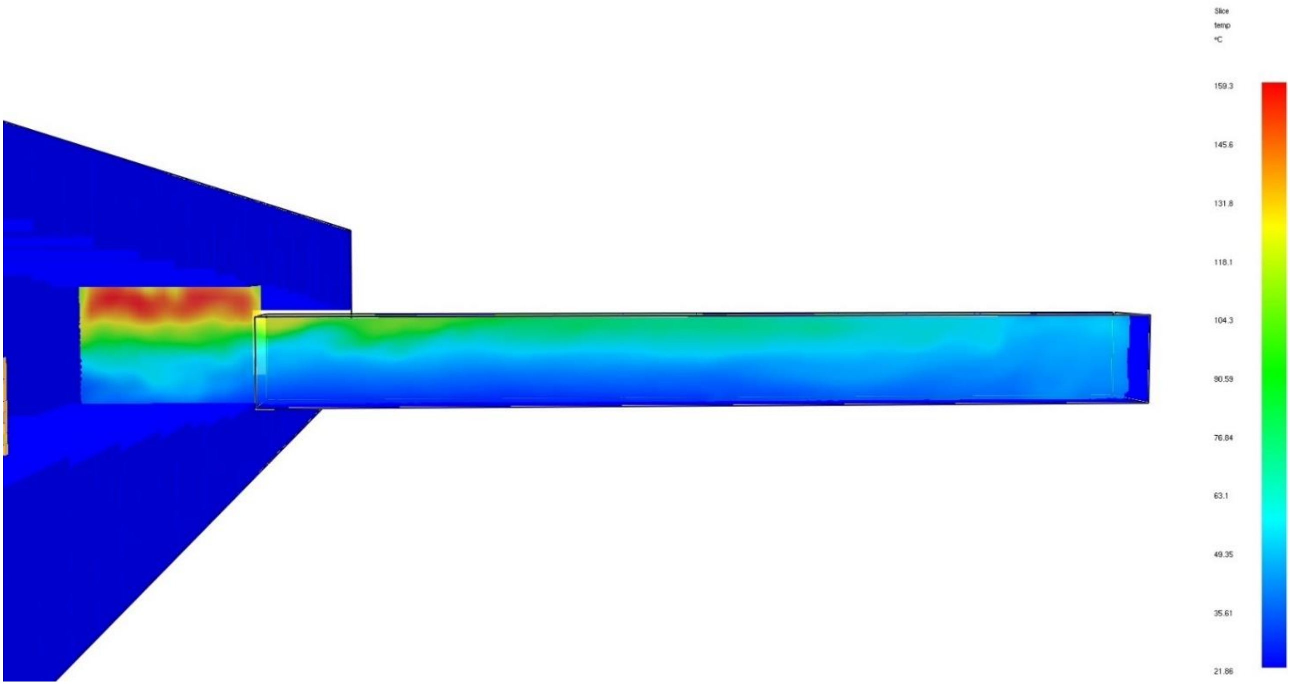

Fig.12. Slice file displaying the temperature variations along the cuddy and in the decline at t=280 s

The variations in visibility can be found in Fig. 13. The visibility rapidly drops to approximately 5.2 m for all positions along the cuddy and the poor visibility can also be seen in the higher CO mass fraction (see Fig. 14) compared with the corresponding mine drift case, i.e. $3.1 \cdot 10^{-5}$ (31 ppm) compared with $2.0 \cdot 10^{-5}$ (20 ppm). The peak mass fraction of CO_2 was approximately 0.016 (16 000 ppm) in the simulation. The poor visibility remains for all positions throughout the entire simulation, whereas the CO mass fraction decreases to below $2 \cdot 10^{-5}$ at the end of the simulation. Thus, the tenability in the cuddy will be worse in the downslope decline case with respect to temperature, visibility and CO/CO_2 mass fraction levels if comparing to the horizontal mine drift case.

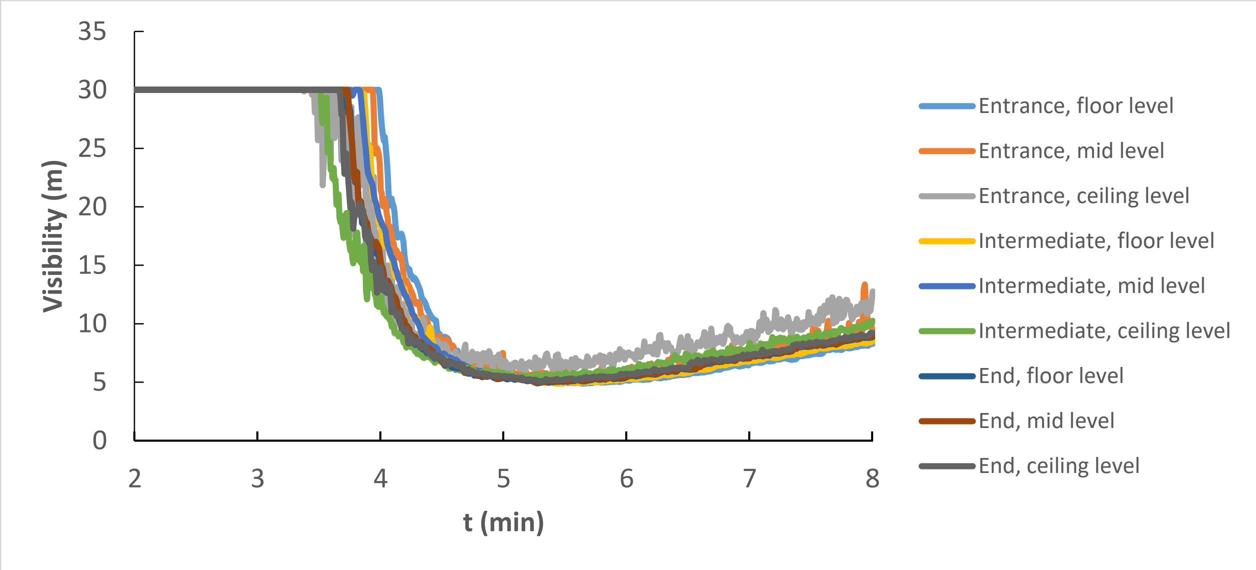

Fig.13. The visibility variations at the entrance, intermediate and end of cuddy at three different heights – downslope decline case

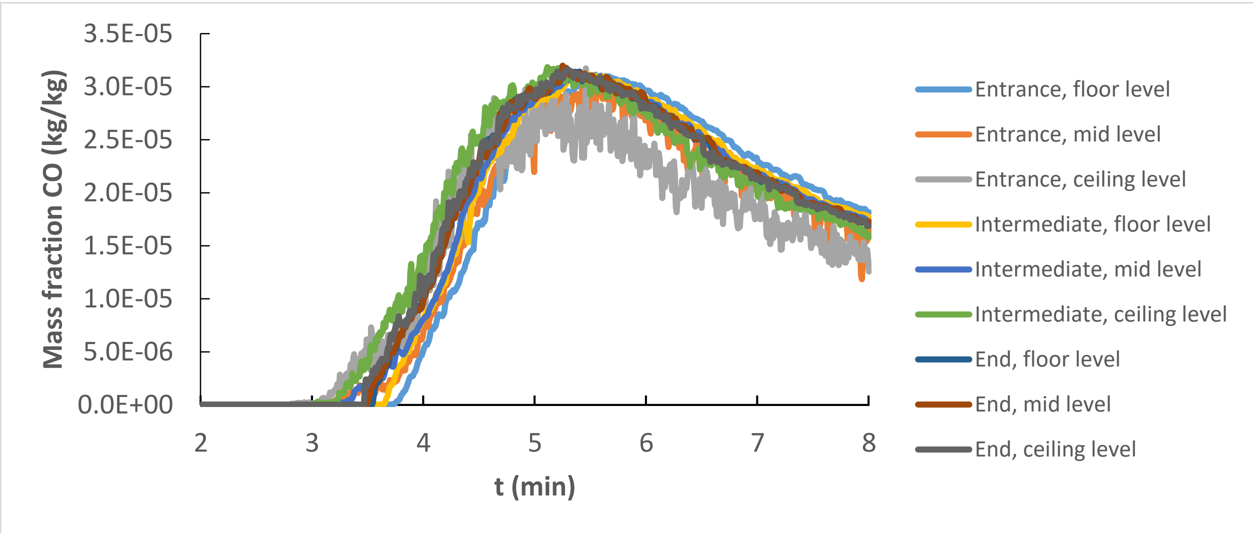

Fig.14. The CO mass fraction variations at the entrance, intermediate and end of cuddy at three different heights – downslope decline case

Upslope decline

The resulting temperatures for the upslope decline scenario can be found in Fig. 15. The temperature distribution is similar to the temperature distributions for the horizontal mine drift scenario and the difference can be found in the magnitude of the temperatures where the temperatures in the cuddy for the upslope decline case is lower than for the mine drift case. Same as for the other two base cases, the highest temperatures at the time of the peak heat release rate can be seen at the ceiling level at the entrance – approximately 50°C - and half-way into the cuddy – approximately 40°C, which is half of the corresponding temperatures in the downslope decline case. The lowest temperatures can be found at the floor level at the entrance and half-way into the cuddy – approximately 25°C, which is very close to the ambient temperature of 22°C. The temperatures at the remaining positions are found around 30°C. These observations are further underlined by studying the slice file in Fig. 16, where the increased stratification and decreased turbulence in the decline results in a thinner smoke layer and where the amount of smoke entering the cuddy will be limited. At the end of the simulation the temperature at the ceiling level at the entrance and half-way into the cuddy is 35-40°C, the average temperature at the floor level at the entrance and half-way into the cuddy is approximately 25°C, and the temperature at the remaining positions is approximately 30°C.

vol. 30, issue 3 / 2024
pp. 1-21

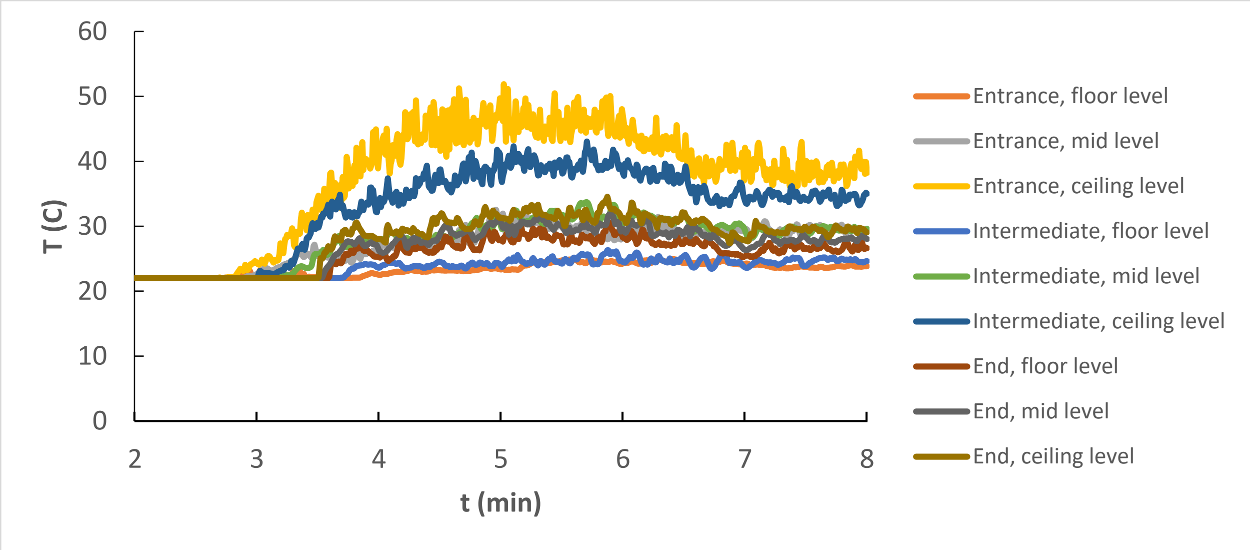

Fig.15. The temperature variations at the entrance, intermediate and end of cuddy at three different heights – upslope decline case

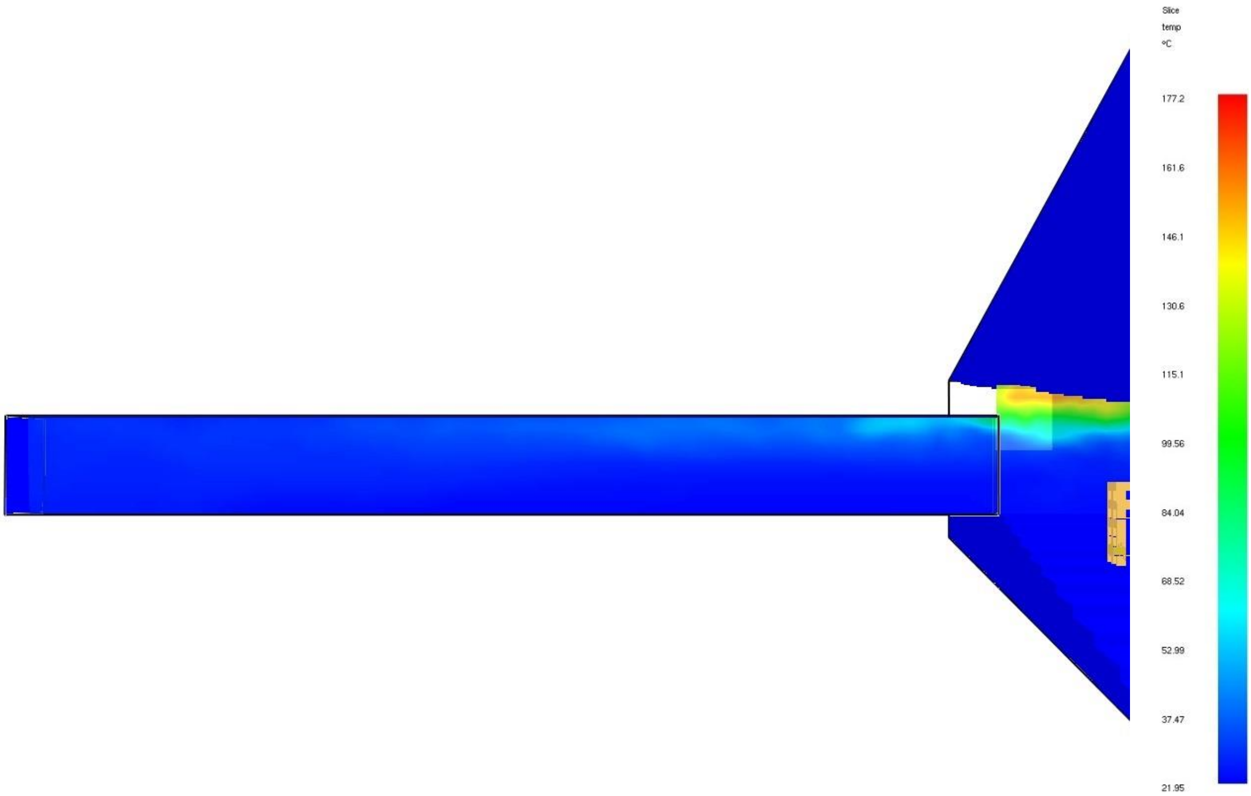

Fig.16. Slice file displaying the temperature variations along the cuddy and in the decline at t=280 s

Fig. 17 displays the visibility variations of the upslope decline case, where the visibility stays above 10 m throughout the entire simulation and where the minimum value was approximately 12 m. At the floor level at the entrance to the cuddy, it is only at the latter part of the simulation that any significant decrease in the visibility could be seen which is due to decreased stratification at the position. The CO mass fraction variations in Fig. 18 displays similar trends, with delayed increase at the floor level at the entrance and with a maximum CO mass fraction of approximately $1.2 \cdot 10^{-5}$ (12 ppm) (compared to $2.0 \cdot 10^{-5}$ for the mine drift case). The maximum CO_2 mass fraction was approximately 0.005 (5 000 ppm) in the simulation. The CO mass fraction decreased to below $1 \cdot 10^{-5}$ for most positions at the end of the simulation. As opposed to the downslope decline case, the tenability in the cuddy in the upslope decline case will be more favourable than in the horizontal mine drift case with respect to temperature, visibility and CO/CO_2 mass fraction levels.

vol. 30, issue 3 / 2024
pp. 1-21

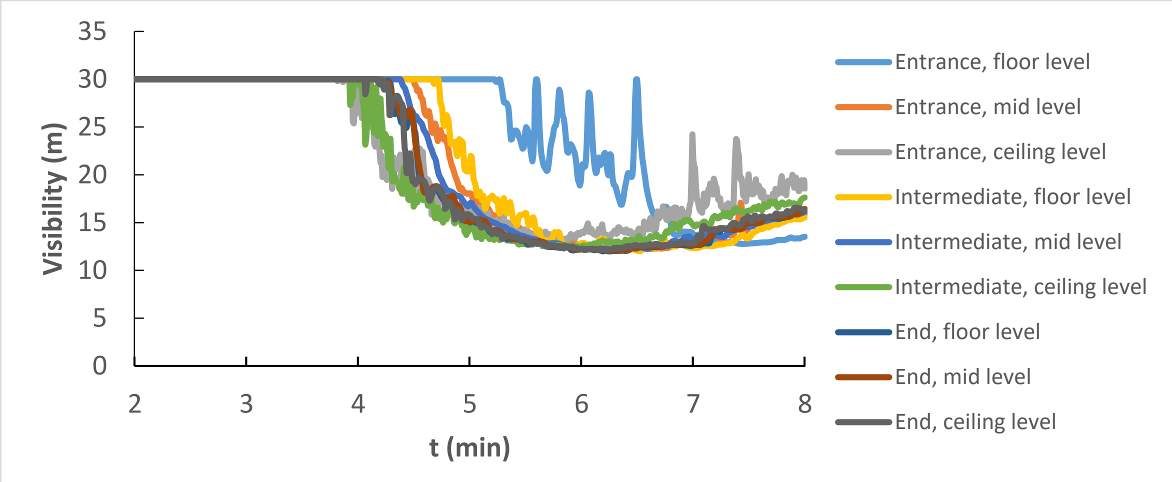

Fig.17. The visibility variations at the entrance, intermediate and end of cuddy at three different heights – upslope decline case

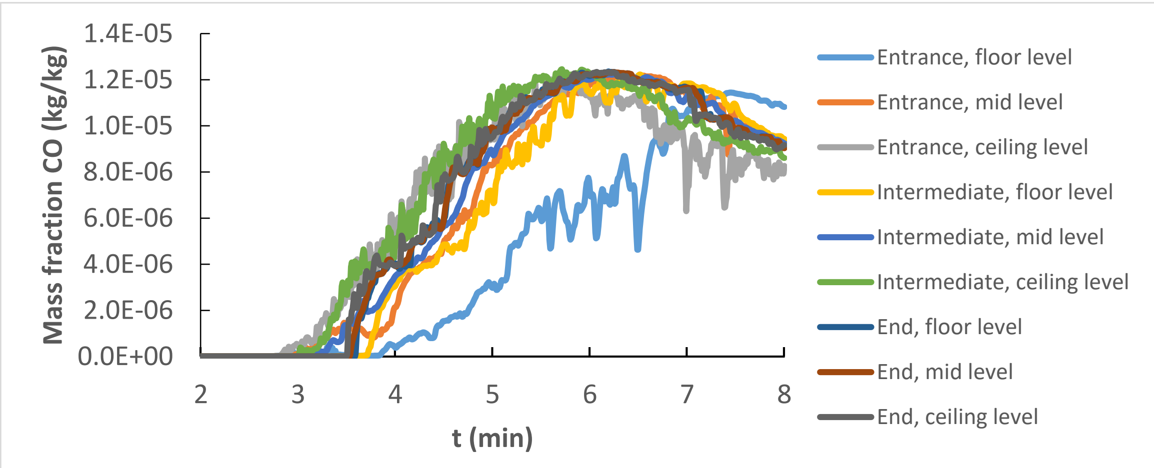

Fig.18. The variations in CO mass fractions at the entrance, intermediate and end of cuddy at three different heights – upslope decline case

4.2 Varying length of cuddy

In the below described simulations the length of the cuddy was increased to 5 m, which corresponds to 75 m in full-scale.

Mine drift

The modelled temperatures were similar to the base case at the entrance and intermediate region of the cuddy, except for the ceiling level which displayed a decrease in temperature. The temperatures at the end of the cuddy were found to be 5-10°C lower at the time of the peak heat release rate compared with the base case. These temperatures correspond to a ~15-25% decrease compared with the base case. The average temperature at the end of the extended cuddy is approximately 30°C during the time of peak heat release rate and approximately 25°C at the end of the simulation. This temperature decrease is significant at the end region of the cuddy and is caused by the increased heat losses of the smoke layer due to an increased, surrounding rock surface along the cuddy.

The differences in visibility are small compared with the base case. The minimum visibility is somewhat higher at approximately 9 m, but still below 10 m. The drop in visibility at the end region of the cuddy occurred at a later stage which was caused by the increased transport time of the smoke layer due to the longer cuddy. The visibility conditions remain more or less constant until the end of the simulation.

The differences in CO mass fractions correspond to the differences in visibility, i.e., the peak mass fraction is somewhat lower than for the base case ($1.7 \cdot 10^{-5}$ compared to $2.0 \cdot 10^{-5}$) and the peak value for the end region of the cuddy occurs later than compared to the base case. The average CO mass fraction decreases to approximately $1.3 \cdot 10^{-5}$ at the end of the simulation. The peak CO_2 mass fraction was approximately 0.0063. The simulation showed generally lower CO/CO_2 mass fractions at the entrance to the cuddy and thus less smoke entered the cuddy which in turn would lead to lower concentrations further into the cuddy.

vol. 30, issue 3 / 2024
pp. 1-21

The conditions at the end region of an extended cuddy will be significantly more favourable with respect to the temperature compared to the base case and to a lesser extent when it comes to visibility and CO/CO_2 mass fractions.

Downslope decline

Same as for the mine drift case, the temperatures at the end of the extended cuddy were significantly lower in the downslope decline case. The temperatures at the end of the cuddy were found to be 10-15°C lower at the time of the peak heat release rate and 10°C lower at the end of the simulation compared with the base case. These temperatures correspond to a ~20-25% and a ~25% decrease compared with the base case. The average temperature at the end of the extended cuddy is below 40°C during the time of peak heat release rate and approximately 30°C at the end of the simulation.

As opposed to the corresponding horizontal mine drift case, the downslope decline case also includes lower temperatures at the end of the simulation. The ceiling temperatures at the entrance and half-way along the extended cuddy decreased to approximately 90°C and 60°C respectively compared with the base case. The floor level temperatures at the entrance and half-way decreased to approximately 35°C.

The differences in visibility are very small compared with the base case. The minimum visibility drops to approximately 5.4 m along the cuddy (compared with approximately 5.2 m for the base case). Same as for the corresponding mine drift case, the drop in visibility occurred at a later stage which was caused by the increased transport time of the smoke layer due to the longer cuddy. At the end of the simulation the visibility stays below 10 m for most positions along the cuddy.

The differences in CO mass fractions correspond to the differences in visibility, i.e., the peak mass fraction along the cuddy is only slightly lower than for the base case ($3.0\cdot10^{-5}$ compared to $3.1\cdot10^{-5}$) and the peak value occurs later than compared to the base case. The CO mass fraction decreases to below $2\cdot10^{-5}$ for most positions at the end of the simulation. The peak mass fraction of CO_2 was approximately 0.013 in the simulation.

The conditions at the end region of an extended cuddy will be more favourable with respect to the temperature compared to the base case but the changes will be negligible when it comes to visibility and CO/CO_2 mass fractions.

Upslope decline

Same as for the other cases, the temperatures at the end of the cuddy were found to be lower. At the time of the peak heat release rate the temperature was approximately 5°C lower at all three positions at the end region compared with the base case (equivalent to a 17% decrease). At the end of the simulation the temperature decrease was approximately 4°C lower at these positions. The average temperature at these positions will be approximately 25°C at the peak heat release rate as well as at the end of the simulation. The ceiling temperature half-way along the cuddy will decrease by approximately 5°C at the peak heat release rate and the end of the simulation. The temperatures at the remaining positions were similar to the corresponding temperatures of the base case.

The differences in visibility were larger compared with the other two cases. The minimum visibility drops to approximately 14 m along the cuddy (compared with approximately 12 m for the base case). The visibility conditions stay more or less constant to the end of the simulation. Same as for the other two cases, the drop in visibility at the end region of the cuddy occurred at a later stage.

Same as for the other two cases, the peak CO mass fraction along the cuddy is only slightly lower than for the base case ($1.1\cdot10^{-5}$ compared to $1.2\cdot10^{-5}$). The CO mass fractions stay more or less constant to the end of the simulation. The peak mass fraction of CO_2 was approximately 0.004 in the simulation.

The conditions at the end region of an extended cuddy will be more favourable with respect to the visibility compared to the base case but the changes will be less significant when it comes to temperature and CO/CO_2 mass fractions.

4.3 Varying distance between cuddy and fire

In the three simulations the distance between the fire and the cuddy was increased to 4 m, which corresponds to 60 m in full-scale.

Mine drift

The resulting modelled temperatures in the cuddy were found to be very close to the corresponding temperatures of the base case. Thus, an increasing distance between the fire and the cuddy will not affect the temperatures encountered in the cuddy. The increased distance will cause an increased cooling and decreased stratification, but the increased amount of smoke entering the cuddy will have a lower temperature, which is seen in the negligible changes in temperature in the cuddy.

vol. 30, issue 3 / 2024
pp. 1-21

The differences in visibility and CO/CO_2 mass fractions were found to be very small. With an increased distance between fire and cuddy the visibility drops slightly – except for the ceiling level at the entrance to the cuddy, where an increase occurs – to a minimum of approximately 7 m (compared to 8 m for the base case). The visibility conditions stay more or less constant to the end of the simulation. The maximum CO mass fraction increases to $2.1 \cdot 10^{-5}$ (compared to $2.0 \cdot 10^{-5}$ for the base case), except for the ceiling level at the entrance where the CO mass fraction decreases. The CO mass fraction decreases to approximately $1.5 \cdot 10^{-5}$ for most positions at the end of the simulation. The peak CO_2 mass fraction was approximately 0.01 in the simulation.

The decreased visibility and increased CO/CO_2 mass fraction is caused by a decreasing stratification (in turn caused by the increased distance to the fire), which will cause a lower height to the smoke layer in the mine drift and an increase in smoke entering the cuddy. At the ceiling level at the entrance to the cuddy, the CO/CO_2 mass fraction will be lower compared to the base case due to a lower degree of stratification in the mine drift.

The conditions at the end region of the cuddy will be slightly less favourable regarding visibility and CO/CO_2 mass fraction compared to the base case, but the differences will be small.

Downslope decline

At the time of the peak heat release rate, generally all the temperatures were significantly lower in the downslope decline case compared with the base case. The temperatures at the end of the cuddy were found to be approximately 10°C lower at the time of the peak heat release rate and the ceiling temperatures at the entrance and half-way through the cuddy were approximately 20°C lower. The temperature differences at the end of the simulation were negligible. These temperatures correspond to a ~15-20% and a ~20-25% decrease compared with the base case. The average temperature at the end of the extended cuddy was approximately 40°C during the time of peak heat release rate.

The decrease in temperature is caused by the increased cooling of the smoke layer due to a longer distance from the fire. A lower degree of stratification contributes to an increased cooling compared with the corresponding horizontal mine drift case. At the end of the simulation – with lower heat release rate and temperatures – the cooling effect will be less significant.

The resulting modelled visibility in the cuddy were found to be very close to the corresponding temperatures of the base case at the time of the peak heat release rate as well as at the end of the simulation. The minimum visibility drops to approximately 5.1 m, compared with approximately 5.2 m for the base case. Thus, an increasing distance between the fire and the cuddy will have little effect on the visibility in the cuddy.

The differences in CO mass fractions correspond to the differences in visibility, i.e., the peak mass fraction is only slightly higher than for the base case ($3.3 \cdot 10^{-5}$ compared to $3.1 \cdot 10^{-5}$). The peak mass fraction of CO_2 was approximately 0.016 in the simulation.

Same as for when extending the length of the cuddy, the conditions in the cuddy will be more favourable with respect to the temperature compared to the base case but the changes will be negligible when it comes to visibility and CO/CO_2 mass fractions.

Upslope decline

The resulting modelled temperatures in the cuddy were found to be very close to the corresponding temperatures of the base case at the time of peak heat release rate and at the end of the simulation. An increasing distance between the fire and the cuddy in an upslope decline case will not affect the temperatures encountered in the cuddy.

The resulting visibility displayed a smaller decrease compared with the corresponding base case. The minimum visibility drops to approximately 11 m, compared with approximately 12 m for the base case. The visibility conditions remain at the same levels towards the end of the simulation.

A slight increase in the CO mass fraction could be detected in the simulation, corresponding to the decrease in visibility. The peak CO mass fraction was approximately ($1.4 \cdot 10^{-5}$ compared to $1.2 \cdot 10^{-5}$). The CO mass fraction decreased to approximately $1.1 \cdot 10^{-5}$ for most positions at the end of the simulation, thus slightly higher than the base case. The peak mass fraction of CO_2 was approximately 0.006 in the simulation.

Compared with the base case, a longer distance to the cuddy in an upslope decline scenario would not affect the temperatures in the cuddy but would result in slightly less favourable conditions with respect to visibility and CO/CO_2 mass fractions.

An upslope decline case will lead to a longer stratification region downstream of the fire and the cooling effect on the smoke layer due to a longer distance between the fire and the cuddy will be lower compared to the downslope decline case.

vol. 30, issue 3 / 2024
pp. 1-21

4.4 Varying heat release rate

In the simulations the peak heat release rate was increased to 46 kW, which corresponds to approximately 40 MW in full-scale. This peak heat release rate corresponds to a very severe fire underground.

Mine drift

The increased heat release rate resulted in increased temperatures across the entire cuddy. At the time of the peak heat release rate the ceiling temperatures at the entrance and half-way through the cuddy increased with approximately 15°C, which corresponds to a 25-30% increase compared with the base case. The corresponding temperature increase at the end region of the cuddy was approximately 5°C, corresponding to an approximate increase of 15%. The temperature increase at the end region of the cuddy persists throughout the entire simulation, whereas the temperature increase at the ceiling level – at the entrance and half-way – was less than 10°C at the end of the simulation. The temperature at the intermediate level half-way through the cuddy displayed similar temperatures as the end region positions, whereas the floor level temperatures at the entrance and half-way through the cuddy were similar to the base case.

The minimum visibility drops to approximately 5.4 m along the cuddy (compared with approximately 8 m for the base case). The visibility conditions remain at approximately the same levels towards the end of the simulation.

Following upon the decreased visibility, the maximum CO mass fraction is increased to $2.9 \cdot 10^{-5}$ (compared to $2.0 \cdot 10^{-5}$ for the base case). The CO mass fraction decreases to approximately $2 \cdot 10^{-5}$ towards the end of the simulation, which is higher than the base case. The peak CO_2 mass fraction was approximately 0.013 in the simulation.

An increasing heat release rate will worsen the conditions along the cuddy considerably with respect to temperature, visibility and CO/CO_2 mass fractions.

Downslope decline

Similar temperature developments as for the mine drift occurred. At the time of the peak heat release rate the ceiling temperatures at the entrance and half-way through the cuddy increased with approximately 30°C, which corresponds to a 30% and a ~40% increase respectively compared with the base case. The corresponding temperature increase at all other positions was approximately 15°C, corresponding to an approximate increase of ~25-30% for the end region. The temperature increase at the end region of the cuddy – and the lower and intermediate level at the entrance and half-way - decreases to approximately 10°C at the end of the simulation. The temperature increase at the ceiling level – at the entrance and half-way – decreases to approximately 15°C at the end of the simulation.

The minimum visibility drops to approximately 3.6 m along the cuddy (compared with approximately 5.2 m for the base case). At the end of the simulation the average visibility has increased to approximately 6 m, which is lower than for the base case (i.e., approximately 9 m).

The peak CO mass fraction increases to $4.9 \cdot 10^{-5}$ (compared to $3.1 \cdot 10^{-5}$ for the base case). The average CO mass fraction decreases to approximately $2.5 \cdot 10^{-5}$ towards the end of the simulation, which is higher than the base case. The peak CO_2 mass fraction was approximately 0.027 in the simulation.

An increased heat release rate will significantly worsen the conditions in the cuddy for a downslope decline case. The changes will be more severe than for the corresponding mine drift case. The worsening conditions will be due to a combination of the increased heat release rate and the higher degree of turbulence in the decline.

Upslope decline

Same as for the other two cases, the temperature increased along the cuddy for an increased heat release rate. At the time of the peak heat release rate the ceiling temperatures at the entrance and half-way through the cuddy increased with approximately 10°C, which corresponds to a 20% and a 25% increase respectively compared with the base case. The corresponding temperature increase at the end region of the cuddy was approximately 5°C, corresponding to an approximate increase of ~15%. The temperature differences at the remaining positions were very small. The temperature increase at the ceiling level – at the entrance and half-way – decreases to approximately 5°C at the end of the simulation. The temperature differences at the remaining positions at the end of the simulation were very small.

The minimum visibility drops to approximately 8 m, compared with approximately 12 m for the base case (thus, dropping below the 10 m threshold). The visibility conditions remain at approximately the same levels towards the end of the simulation.

The peak CO mass fraction increases to $2 \cdot 10^{-5}$ (compared to $1.2 \cdot 10^{-5}$ for the base case). The average CO mass fraction decreases to approximately $1.5 \cdot 10^{-5}$ towards the end of the simulation, thus still higher than the base case. The peak CO_2 mass fraction was approximately 0.008 in the simulation.

An increased heat release rate will therefore worsen the conditions in the cuddy for an upslope decline case. The changes will be less severe than for the corresponding downslope decline case. The less worsening conditions will be due to a lower degree of turbulence and a higher degree of stratification in the decline.

4.5 Varying degree of inclination

In the following two simulations the inclination was increased from 5% to 10%. As the inclination is a dimensionless parameter, the full-scale inclination will be identical with the modelled model-scale inclination.

Downslope decline

The increased inclination resulted in significant temperature increases at the ceiling level at the entrance of the cuddy, where the temperature increase is approximately 20°C compared to the base case at the time of peak heat release rate. This corresponds to a 20% temperature increase compared to the base case. The corresponding temperature differences for the remaining positions are very small compared to the base case and will persist throughout the remaining simulation. The temperature difference at the ceiling entrance position decreases to approximately 10°C at the end of the simulation. The increased inclination will result in a further increased turbulence in the decline, leading to hotter gas volumes entering the cuddy at the ceiling level. Still, the impact on the resulting temperatures at the end region of the cuddy is very small. Fig. 19 displays the slicefile with the temperature distribution at the time of the peak heat release rate. When comparing with the temperature distribution in Fig. 12, the stratification decreased with increasing inclination and resulted in hotter gas volumes at lower heights in the decline.

The minimum visibility drops to approximately 5.8 m, compared with approximately 5.2 m for the base case. Thus, dropping below the 10 m threshold but slightly better conditions compared to the base case. The average visibility increases to approximately 10 m towards the end of the simulation, which is equivalent to the base case.

The peak CO mass fraction decreases to $3.0 \cdot 10^{-5}$ (compared to $3.1 \cdot 10^{-5}$ for the base case). The average CO mass fraction decreases to approximately $1.5 \cdot 10^{-5}$ towards the end of the simulation, thus lower than the base case. The peak CO_2 mass fraction was approximately 0.016 in the simulation.

An increased inclination will therefore have very little impact on the conditions in the cuddy for a downslope decline case. The only noticeable difference will be the increased temperatures at the ceiling level at the entrance of the cuddy.

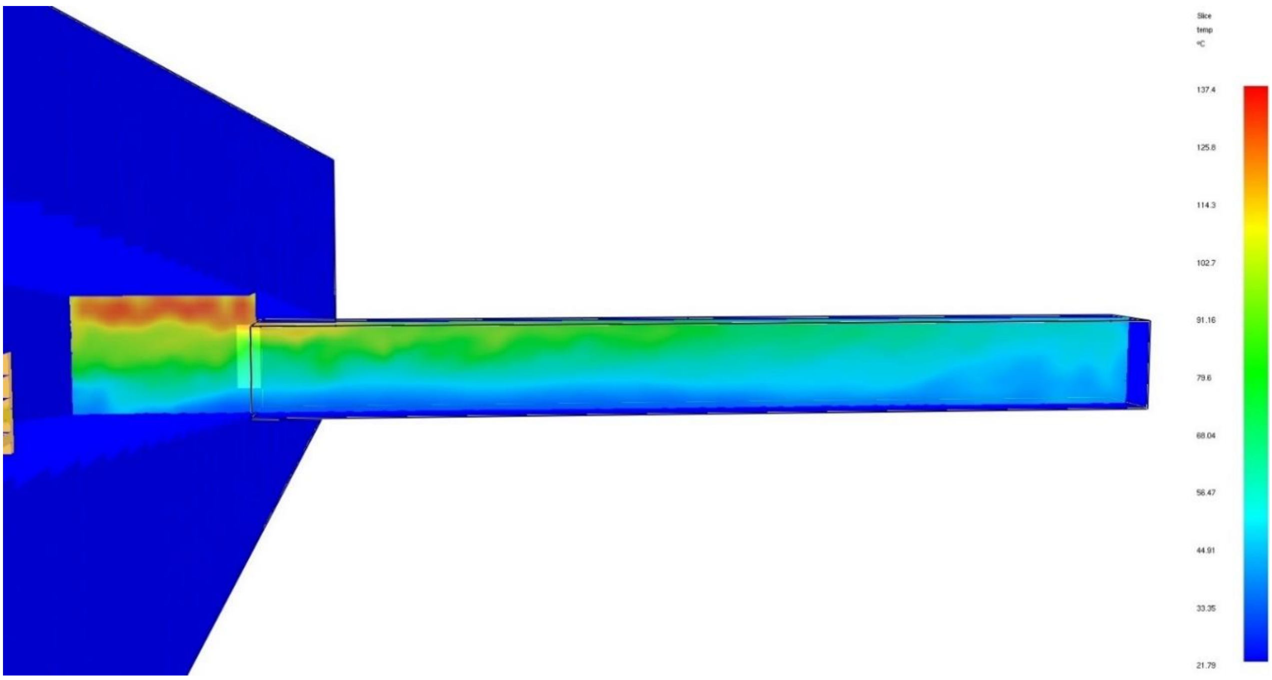

Fig.19. Slice file displaying the temperature variations along the cuddy and in the decline at t=280 s

vol. 30, issue 3 / 2024
pp. 1-21

Upslope decline

The increased inclination resulted in temperature increases at the end region of the cuddy, where the temperature increase was approximately 5°C compared to the base case at the time of peak heat release rate. This corresponds to an approximately 15% temperature increase compared to the base case. The corresponding temperature differences for the remaining positions were approximately 10°C compared to the base case, corresponding to a significant temperature increase at the floor level at the entrance and half-way into the cuddy (i.e., a 40% increase) and a 20-25% increase at the ceiling level at the entrance and half-way into the cuddy. The corresponding temperature differences at the end of the simulation were found to be very small for all positions along the cuddy. Fig. 20 displays the slicefile with the temperature distribution at the time of the peak heat release rate. When comparing with the temperature distribution of the base case (Fig. 16), the increased inclination will cause a decreased stratification in the upslope decline case as well. With decreased stratification, hotter gas volumes can be found at lower heights in the decline and with a larger portion of hot gases entering the cuddy.

The minimum visibility drops to approximately 12 m, which is identical with the minimum visibility for the base case. The visibility conditions improved significantly towards the end of the simulation with an average visibility of approximately 20 m, which is considerably higher than the base case.

The peak CO mass fraction was approximately $1.2 \cdot 10^{-5}$, which is identical with the peak value of the base case. The average CO mass fraction decreases to approximately $0.7 \cdot 10^{-5}$ towards the end of the simulation, slightly lower than the base case. The peak CO_2 mass fraction was approximately 0.006 in the simulation.

An increased inclination will therefore have negligible impact on the visibility and CO/CO_2 mass fraction conditions in the cuddy for an upslope decline case. The only noticeable difference will be the increased temperatures at the entrance region and half-way through the cuddy.

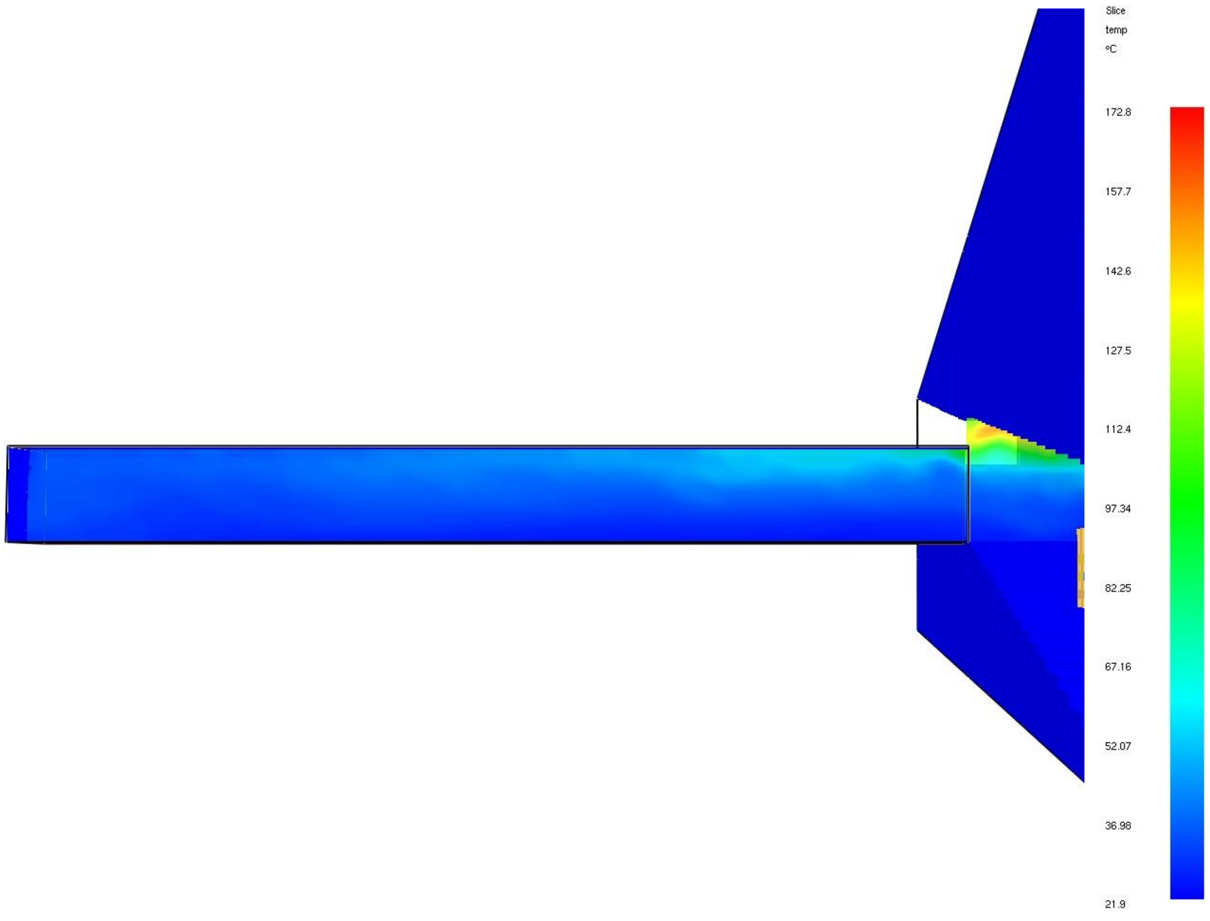

Fig.20. Slice file displaying the temperature variations along the cuddy and in the decline at t=280 s

4.6. Varying longitudinal flow velocity

In the simulations the longitudinal ventilation velocity was increased to 0.516 m/s, which corresponds to approximately 2 m/s in full-scale.

Mine drift

The increased ventilation velocity resulted in increased temperatures across the entire cuddy at the time of the peak heat release rate. At the time of the peak heat release rate the ceiling temperatures at the entrance and half-way through the cuddy increased with approximately 15°C, which corresponds to a 25-30% increase compared with the base case. The corresponding temperature increase at the end region of the cuddy was approximately 10°C, corresponding to an approximate increase of 30%. The corresponding temperature increase at the remaining positions was approximately 15°C. The temperatures at the end of the simulation were similar to the base case for all positions. Fig. 21 displays the slicefile with the temperature distribution at the time of the peak heat release rate. When comparing with the temperature distribution of the base case (Fig. 8), the increased ventilation velocity will cause an increased turbulence, a decreased stratification, and hotter gas volumes found at lower heights in the mine drift and larger portions of hot gases entering the cuddy.

The minimum visibility drops to approximately 10 m, compared with approximately 8 m for the base case. At the end of the simulation the visibility was found to be significantly better than for the base case, with the visibility ranging from 20 m to 30 m.

The maximum CO mass fraction was found to be $1.6\cdot10^{-5}$, compared to $2.0\cdot10^{-5}$ for the base case. At the end of the simulation the CO mass fraction decreases even further compared to the base case, with average values around $7\cdot10^{-6}$. The peak CO_2 mass fraction was approximately 0.009 in the simulation.

An increasing longitudinal ventilation velocity will worsen the conditions along the cuddy with respect to temperature but will improve the conditions with respect to visibility and CO/CO_2 mass fractions.

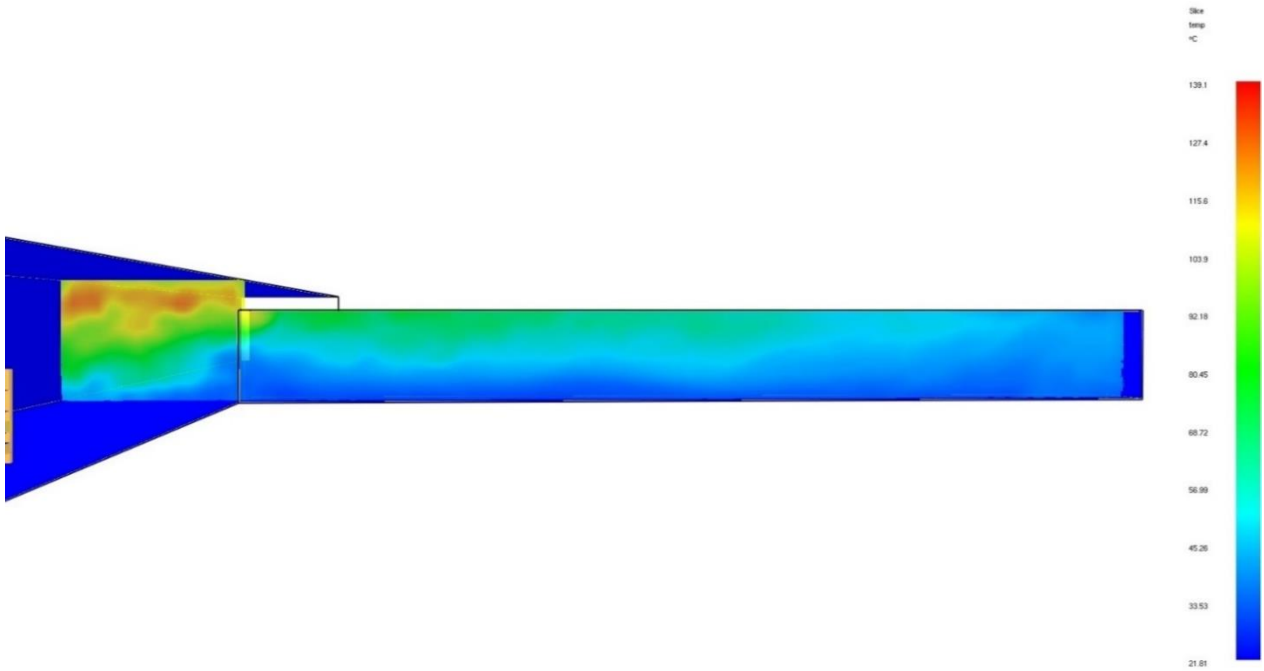

Fig. 21. Slice file displaying the temperature variations along the cuddy and in the mine drift at t=280 s

Downslope decline

The increased ventilation velocity resulted in decreased temperatures across the entire cuddy at the time of the peak heat release rate as well as at the end of the simulation. At the time of the peak heat release rate the average temperature decrease for all positions along the cuddy was approximately 5°C, corresponding to an approximately 10% decrease for the end region and an approximately 5% decrease for the ceiling level at the entrance and half-way through the cuddy. The temperature decrease was more significant at the end of the simulation with an approximately 15°C decrease for the ceiling level at the entrance and half-way and a 10°C decrease for the remaining positions. The increased ventilation velocity in the downslope decline case will cause a decrease in the stratification, but also an increased mixing – due to increased turbulence - and cooling of the flowing gas volumes and decreasing gas volume temperatures entering the cuddy.

The minimum visibility drops to approximately 10 m, compared with approximately 5.2 m for the base case. At the end of the simulation the visibility was increased more than for the base case, with the visibility ranging from 15 m to 20 m.

The maximum CO mass fraction – occurring at the time of the peak heat release rate - was found to be $1.6\cdot10^{-5}$, compared to $3.1\cdot10^{-5}$ for the base case. At the end of the simulation the CO mass fraction is still lower compared to the base case, with average values around $0.8 \cdot 10^{-5}$. The peak CO_2 mass fraction was approximately 0.01 in the simulation.

An increasing longitudinal ventilation velocity will improve the conditions along the cuddy with respect to temperature and significantly with respect to visibility and CO/CO_2 mass fractions.

Upslope decline

The increased ventilation velocity resulted in increased temperatures across the entire cuddy at the time of the peak heat release rate. At the time of the peak heat release rate the ceiling temperatures at the entrance and half-way through the cuddy increased with approximately 20°C, which corresponds to a 40-50% increase compared with the base case. The corresponding temperature increase at the end region of the cuddy was approximately 10°C, corresponding to an approximate increase of 30%. The corresponding temperature increase at the remaining positions was approximately 15°C. The temperatures at the end of the simulation were similar to the base case for all positions. Same as for the mine drift case, an increased ventilation velocity will cause an increased turbulence, a decreased stratification, and hotter gas volumes found at lower heights in the decline and larger portions of hot gases entering the cuddy.

The minimum visibility drops to approximately 12 m, which is identical with the base case. At the end of the simulation the visibility was found to be 5 m higher for all positions compared to the base case.

The maximum CO mass fraction – occurring at the time of the peak heat release rate - was found to be $1.2 \cdot 10^{-5}$, which is identical with the base case. At the end of the simulation the CO mass fraction is slightly lower at all positions compared to the base case (i.e., resulting in an approximate decrease of $0.2 \cdot 10^{-5}$). The peak CO_2 mass fraction was approximately 0.007 in the simulation.

An increasing longitudinal ventilation velocity will worsen the conditions along the cuddy with respect to temperature but will not change or display very small changes with respect to visibility and CO/CO_2 mass fractions.

4.7. Ranking of the fire scenarios – tenability

Studying the temperature at the end region at the time of the peak heat release rate, the minimum visibility, and the peak CO mass fraction, the individual scenarios were ranked with respect to the tenability.

In the case of the mine drift, the scenario with the extended cuddy length resulted in the best tenability conditions, whereas the scenario with the increased heat release rate resulted in the worst conditions.

Regarding the downslope decline case, the scenario with the extended cuddy length and the scenario with increased ventilation velocity resulted in the best conditions. Again, the scenario with the increased heat release rate resulted in the worst conditions.

For the upslope decline case, the scenario with the extended cuddy length resulted in the best tenability conditions, whereas the scenario with the increased heat release rate and the scenario with increased ventilation velocity resulted in the worst conditions.

The overall best conditions were found for the upslope decline case with an extended cuddy length. The overall worst conditions were found for the downslope decline case with an increased heat release rate.

If varying multiple parameters, the conditions can be further improved or worsened. For example, in the case of a downslope decline, an extended cuddy in conjunction with an increased ventilation velocity will result in further improved conditions.

4.8. Mitigating measures

Given the results from the simulations, additional mitigating measures – taken prior to or during a fire – to increase the tenability in the cuddy can also be deduced from the findings.

If possible and practically feasible, a partition covering the entire cross-section of the cuddy would significantly reduce or possibly fully prevent – depending on the structural integrity of the partition - the smoke from entering the cuddy. The partition could be positioned at a distance from the entrance to take advantage of the cooling of the smoke along the cuddy and increase the probability of the partition successfully blocking the smoke.

If a full cross-sectional partition is not possible or practical, a screen at the upper portion of the cuddy entrance could be a mitigating measure. The screen would foremost reduce the amount of hot gases at the ceiling from entering the cuddy. If the cuddy is long, additional screens could be installed further into the cuddy to decrease the risk of hot gases slipping through to the end region of the cuddy.

A further mitigating measure would be taking advantage of the occurring flow separation and eddy formation downstream of a protruding rock section, which is positioned directly upstream of the entrance to

vol. 30, issue 3 / 2024
pp. 1-21

the cuddy (see Fig. 22). The flow of smoke – occurring at the flow separation – will be marked by instability and large energy dissipation [16]. The measure would decrease the inflow of smoke into the cuddy and could also be combined with a screen at the cuddy ceiling.

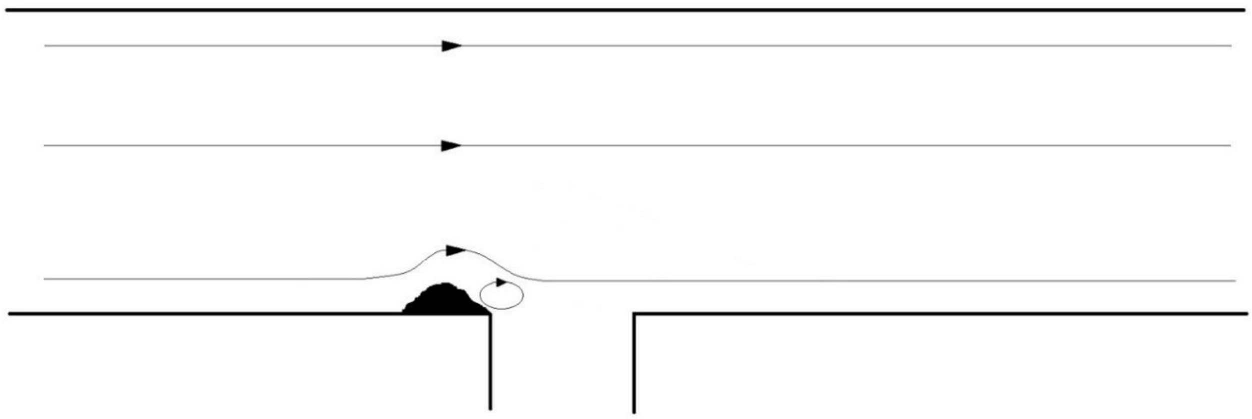

Fig.22. Flow separation and eddy formation downstream of a protruding rock. The flow in the mine drift or decline is seen from above and with a cuddy perpendicular to the mine drift/decline

Varying the ventilation flow velocity in the mine drift or decline could also be used as a mitigating tool. Given the results from the simulations, mitigating measure with respect to the ventilation velocity will differ somewhat between the cases. In the case of a mine drift the visibility and CO/CO_2 mass fractions conditions will improve if increasing the ventilation velocity, but the temperature will increase in the cuddy. An increased ventilation velocity combined with a screen at the cuddy ceiling could possibly be a mitigating measure for the mine drift case. In the case of a downslope decline the temperature, visibility as well as CO/CO_2 mass fraction conditions improved with increasing ventilation velocity and would therefore be a good option. In the case of an upslope decline the temperature conditions worsened while the visibility and CO/CO_2 mass fraction conditions did not change. A decreased ventilation velocity could therefore be a good option in the case of an upslope decline.

5. Conclusions

A parametric study was conducted on the sheltering effect of a cuddy during a fire in an underground mine. Experimental data from fire experiments in a model-scale mine drift and modelling results from a CFD model were used when analyzing the impact of various parameters on the conditions in a cuddy with a fire ongoing in an adjacent horizontal mine drift, downslope decline and an upslope decline.

When increasing the length of the cuddy the conditions (i.e., the temperature at the end region of the cuddy, visibility and CO/CO_2 mass fractions) for all three cases improved. The temperature decrease is caused by the increased heat losses of the smoke layer due to an increased, surrounding rock surface along the cuddy.

If increasing the distance between the fire and the cuddy entrance, the simulation results only showed minor or negligible changes in the conditions. In the case of the mine drift the increased distance will cause a decreased stratification and increased cooling, but the decreased smoke temperature will be nullified by the increased amount of smoke entering the cuddy.

An increased heat release rate will in all three cases result in significantly worsened conditions.

An increased inclination in the two decline cases led to only minor or negligible changes.

When increasing the ventilation flow velocity in the mine drift or decline, the visibility and CO/CO_2 mass fraction conditions will improve in a cuddy adjacent to a mine drift but will worsen with respect to the temperature. The increased ventilation velocity will cause an increased turbulence, a decreased stratification, and hotter gas volumes found at lower heights in the mine drift and larger portions of hot gases entering the cuddy. For a downslope decline case the temperature, visibility as well as CO/CO_2 mass fraction conditions will all improve. The increased ventilation velocity will cause a decrease in the stratification, but also an increased mixing – due to increased turbulence - and cooling of the flowing gas volumes and decreasing gas volume temperatures entering the cuddy. For an upslope decline case the temperature conditions worsened while the visibility and CO/CO_2 mass fraction conditions did not change. The reason behind the temperature increase was identical with the corresponding mine drift case.

For the mine drift case, extending the cuddy length resulted in the best tenability conditions and increasing the heat release rate resulted in the worst conditions.

vol. 30, issue 3 / 2024
pp. 1-21

In the downslope decline case, extending the cuddy length or increasing the ventilation velocity resulted in the best conditions. An increased heat release rate resulted in the worst conditions.

For the upslope decline case, extending the cuddy length resulted in the best conditions and increasing the heat release rate or increasing the ventilation velocity resulted in the worst conditions.

The results from the study will increase the understanding of the impact of various influencing parameters on the sheltering effect of a cuddy and will improve the safety of the underground personnel during the evacuation phase of an occurring fire underground.

References

[1] **Hansen, R., Ingason, H.** 2012.
Heat release rates of multiple objects at varying distances. Fire Safety Journal, vol.52, pp. 1–10.

[2] **Edwards, J.C., Hwang, C.C**. 1999.
CFD Analysis of Mine Fire Smoke Spread and Reverse Flow Conditions. Proceedings of the Eighth US Mine Ventilation Symposium, Rolla, Missouri, June 11-17, 1999, pp 417-422

[3] **Friel, G.F., Yuan, L., Edwards, J.C., Franks, R.A**. 2006.
Fire-generated smoke rollback through crosscut from return to intake - experimental and CFD study. NIOSH.

[4] **Jaszczur, M., Karch, M., Zych, M., Hanus, R., Petryka, L., Świsulski, D**. 2016.
Air flow phenomena in the model of the blind drift. EPJ Web of Conferences 114, 02148

[5] **Chen, L., Mao, P., Zhang, Y., Xing, S., Li, T**. 2020.
Experimental study on smoke characteristics of bifurcated tunnel fire. Tunnelling and Underground Space Technology, vol 98.

[6] **Hansen R**. 2022.
The throttle effect – blower fan versus exhaust fan. Revista Minelor – Mining Revue, vol 28, pp 1-20.

[7] **Wu Y, Atkinson GT, Stoddard JP, James P**. 1997.
Effect of Slope on Control of Smoke Flow in Tunnel Fires. Proceedings of 5th Int. Conf. on Fire Safety Science, Melbourne, Australia, pp 1225-1236.

[8] **Hansen, R**. 2021.
Modelling the throttle effect in a mine drift. Journal of Sustainable Mining, vol. 20, pp. 277-295.

[9] **Hansen, R., Ingason, H**. 2010.
Model scale fire experiments in a model tunnel with wooden pallets at varying distances. Research report SiST 2010:8. Mälardalen University. Västerås, Sweden.

[10] **Yeoh, G.H., Yuen, K.K**. 2009.
Computational Fluid Dynamics in Fire Engineering, Theory, Modelling and Practice. Academic Press, Oxford.

[11] *** * ***, 2000
SFPE Engineering Guide to Performance-Based Fire Protection. Society of Fire Protection Engineers, Bethesda, Maryland

[12] **Heskestad, G**. 1972.
Modeling of Enclosure Fires. Proceedings of the Fourteenth Symposium (International) on Combustion, 1021-1030, The Pennsylvania State University, USA.

[13] **Quintiere, J.G**. 1989
Scaling Applications in Fire Research. Fire Safety Journal, vol 15, pp 3-29.

[14] *** * ***, 2014
New Zealand Building Code Handbook. Ministry of Business, Innovation and Employment, Wellington

[15] *** * ***, 2023
NFPA 130, Standard for Fixed Guideway Transit and Passenger Rail Systems. National Fire Protection Association, Quincy

[16] **Vennard, J.K., Street, R.L**. 1982.
Elementary fluid mechanics. John Wiley & Sons